

Distributed Circumnavigation Using Bearing Based Control with Limited Target Information

Kushal P. Singh¹, Member, IEEE, Manvi Bengani², Darshit Mittal³, Twinkle Tripathy⁴, Senior Member, IEEE

Abstract—In this paper, we address the problem of circumnavigation of a stationary target by a heterogeneous group comprising of n autonomous agents, having unicycle kinematics. The agents are assumed to have constant linear speeds, we control only the angular speeds. Assuming limited sensing capabilities of the agents, in the proposed framework, only a subset of agents, termed as *leaders*, know the target location. The rest, termed as *followers*, do not. We propose a distributed guidance law which drives all the agents towards the desired objective; global asymptotic stability (GAS) is ensured by using Zubov's theorem. The efficacy of the approach is demonstrated through both numerical simulations and hardware experiments on the TurtleBots utilising OptiTrack motion capture system.

I. INTRODUCTION

Cooperative circumnavigation is a fundamental problem in applications like surveillance [1], reconnaissance [2], environmental monitoring [3] and multi-robot firefighting [4]. Unicycle agents are widely used to achieve such tasks. They have inherent non-holonomic kinematic constraints and are underactuated; yet, their use is motivated from the fact that they are simplified representations of several realworld vehicles.

When working as stand-alone systems, classical single-agent based circumnavigation approaches typically exploit range information [5]–[9] or bearing information [10]. While single-agent solutions are useful, multi-agent coordination based approaches offer scalability, fault tolerance, and reduced sensory requirements. Cyclic pursuit based multi-agent approaches for circumnavigation have been widely investigated, from early Lyapunov-based cyclic formations under limited communication [11] to rotationally invariant formations involving heterogeneous agent speeds [12], [13]. Recently, the authors in [14] addressed local stability issues for unicycles with constant, identical linear speeds.

Further studies have explored more diverse formations. Using leader-follower based strategies for agents modelled as integrators, the authors in [15] propose strategies to achieve circular and elliptical formations. Distributed strategies for desired circular path generation using dynamic unicycles is

explored in [16]. For heterogeneous agents, recent works have also focused on classifying motion regimes [17], controlling only angular speeds or utilising attractive-repellent behaviours by controlling both linear and angular velocities [18].

In scenarios with limited target information availability, the authors in [19], [20] developed laws for cyclic and directed spanning-tree communication graphs among agents modelled as unicycles, succeeding even when one (root) agent tracks the target. The authors in [21] introduced a distributed estimator-based method by controlling both linear and angular speeds to maintain desired radii.

Several of the afore-mentioned works require distance measurements or even provide local stability guarantees even by controlling both linear and angular speeds. In this paper, we address the problem of circumnavigation without distance measurements while also guaranteeing system stability. Moreover, we control only the angular speeds of the agents with unicycle kinematics, thereby, facilitating an easier realworld implementation [14]. Our major contributions are summarised as follows:

- *Bearing based distributed guidance law*: We present a bearing based distributed guidance law that guarantees circumnavigation of a stationary target by a group of n heterogeneous autonomous agents, by controlling only angular speeds. The proposed guidance law is distributed in the sense that the target's location is known only to a few agents. The use of bearing information and a memoryless design further simplifies its implementation.
- *Global asymptotic stability*: The proposed distributed guidance law design ensures circumnavigation by the entire group from any arbitrary initial conditions. GAS is established using Zubov's theorem [22].
- *Hardware implementation*: The applicability of the proposed distributed guidance law is demonstrated through realworld experiments performed using TurtleBot robots.

The remainder of the paper is organised as follows: Section II provides the necessary preliminaries, and Section III details the problem formulation. The proposed guidance law is presented in Section IV. The approach is validated through numerical simulations in Section V and hardware experiments in Section VI. Finally, Section VII concludes the paper.

II. PRELIMINARIES

Graph theory: A directed graph $\mathcal{G} = (\mathcal{V}, \mathcal{E})$, where $\mathcal{V} = \{1, 2, \dots, n\}$ represents the set of nodes (agents) and $\mathcal{E} \subseteq$

* This work was not supported by any organisation.

* All the authors are affiliated with the Indian Institute of Technology, Kanpur-208016, India.

¹K. P. Singh is a research scholar, ²M. Bengani is an undergraduate student, and ⁴T. Tripathy is an assistant professor with the Department of Electrical Engineering.(e-mail: kushalp20, manvib22, ttripathy@iitk.ac.in).

³D. Mittal is an undergraduate student in the Department of Mechanical Engineering.(e-mail: darshitm23@iitk.ac.in).

$\mathcal{V} \times \mathcal{V}$ represents the set of edges (communication links). The edge $(i, j) \in \mathcal{E}$ denotes an outgoing edge from node i to node j ; then, node j becomes the out-neighbour of node i and node i the in-neighbour of node j . A node with no outgoing edges is called a *sink node*. Within this framework, the existence of such a link implies that agent i can sense the heading angle of agent j and the LOS angle from agent i to j . A digraph \mathcal{G} is called *strongly connected* if there exists a directed path from any node to every other node. A digraph \mathcal{G} is *weakly connected* if the undirected version of \mathcal{G} is connected.

Nonlinear systems: A nonlinear system is represented as $\dot{x} = f(t, x, u)$, where $f : D \rightarrow \mathbb{R}^n$ and D is the domain. We refer to x as the state, t as time and u as the input. It is referred to as an autonomous system if $\dot{x} = f(x)$. The equilibrium point ($x = 0$) of $\dot{x} = f(x)$ is:

- Stable if for each $\epsilon > 0$, there exist $\delta = \delta(\epsilon) > 0$ such that $\|x(0)\| < \delta \implies \|x(t)\| < \epsilon, \forall t \geq 0$.
- Asymptotically stable if it is stable and δ can be chosen such that $\|x(0)\| < \delta \implies \lim_{t \rightarrow \infty} x(t) = 0$.
- GAS if it is asymptotically stable and domain $D = \mathbb{R}^n$.

Lemma 1: (Zubov's Theorem) Consider the non-linear system $\dot{x} = f(x)$ with an equilibrium at the origin and let $G \subset \mathbb{R}^n$ be a domain containing the origin. Suppose there exist two functions $V : G \rightarrow \mathbb{R}$ and $h : \mathbb{R}^n \rightarrow \mathbb{R}$ with the following properties:

- V is continuously differentiable and positive definite in G and satisfies

$$0 < V(x) < 1, \quad \forall x \in G \setminus \{0\}. \quad (1)$$

- As x approaches the boundary of G , or in case of unbounded G as $\|x\| \rightarrow \infty$, $\lim V(x) = 1$.
- h is continuous and positive definite on \mathbb{R}^n .
- For $x \in G$, $V(x)$ satisfies the partial differential eqn.

$$\frac{\partial V}{\partial x} f(x) = -h(x)[1 - V(x)]. \quad (2)$$

Then, $x = 0$ is asymptotically stable and G is the region of attraction (ROA).

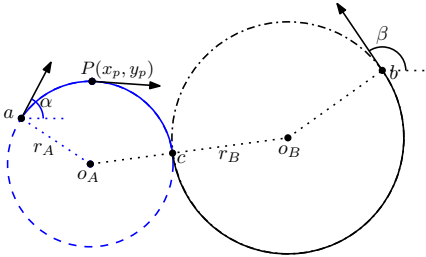


Fig. 1: Location of centres \mathbf{o}_A and \mathbf{o}_B of circles \mathcal{C}_A and \mathcal{C}_B , respectively

Consider the traversal problem of an autonomous vehicle starting and ending at pre-specified oriented points $A(\mathbf{a}, \alpha)$ and $B(\mathbf{b}, \beta)$, respectively. Suppose the traversal is along two circles \mathcal{C}_A & \mathcal{C}_B of radii r_A & r_B , which are tangent to each other, as depicted in Fig. 1. The coordinates of the centres \mathbf{o}_A and \mathbf{o}_B are given by $\mathbf{o}_A = (a_x + r_A \sin \alpha, a_y - r_A \cos \alpha)$ and $\mathbf{o}_B = (-r_B \sin \beta, r_B \cos \beta)$, respectively. The specification of such a circle-circle (CC) trajectory is as given below:

Lemma 2: [23] For any values of the oriented points $A(\mathbf{a}, \alpha)$ and $B(\mathbf{b}, \beta)$, a unique CC trajectory exists $\forall r_A \in \mathbb{R}$ such that r_B is given by $r_B = p_3/(r_A - p_1) + p_2$ where:

$$p_1 = (a_x \sin \beta - a_y \cos \beta)/(1 - \cos(\alpha - \beta)),$$

$$p_2 = (a_x \sin \alpha - a_y \cos \alpha)/(1 - \cos(\alpha - \beta)),$$

$$p_3 = \left(\frac{a_x \sin((\alpha + \beta)/2) - a_y \cos((\alpha + \beta)/2)}{1 - \cos(\alpha - \beta)} \right)^2.$$

III. PROBLEM FORMULATION

Circumnavigation is described as agents moving in circular paths around a central target, as illustrated in Fig. 2a. Such motions are critical in various applications ranging from surveillance and reconnaissance to environmental monitoring and multi-robot firefighting. Motivated by these applications, in this work, we explore the design of distributed guidance laws for autonomous vehicles to achieve circumnavigation around a fixed target point.

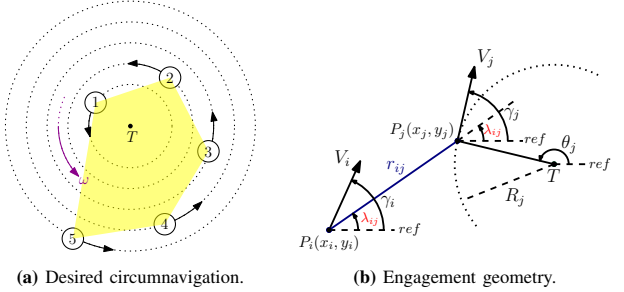


Fig. 2

We begin by considering a group of n heterogeneous autonomous agents connected over a digraph $\mathcal{G}(\mathcal{V}, \mathcal{E})$ and modelled as unicycles. A unicycle is a simplified representation of several real-world systems like cars, fixed-wing aircrafts, submarines, etc. and, hence, are widely used in the guidance and control literature. The kinematics of such an agent is described by:

$$x_j = v_j \cos \gamma_j, \quad y_j = v_j \sin \gamma_j, \quad \dot{\gamma}_j = u_j, \quad (3)$$

where $j \in \{1, 2, \dots, n\} = \mathcal{V}$, $P_j(x_j, y_j) \in \mathbb{R}^2$ are the position coordinates, $\gamma_j \in \mathbb{S}^1$ is its heading angle, $v_j \in \mathbb{R}$ is the constant forward speed and $u_j \in \mathbb{R}$ is the angular control input. In the given framework, we aim to achieve the desired objective by controlling only u_j and keeping v_j constant. This facilitates the practical implementability of the results. However, it makes the problem more challenging by further under-actuating the system.

The spatial geometry in polar coordinates between any two agents i and j is given by:

$$\dot{r}_{ij} = v_j \cos(\gamma_j - \lambda_{ij}) - v_i \cos(\gamma_i - \lambda_{ij}) \quad (4a)$$

$$r_{ij} \dot{\lambda}_{ij} = v_j \sin(\gamma_j - \lambda_{ij}) - v_i \sin(\gamma_i - \lambda_{ij}), \quad (4b)$$

where r_{ij} is the distance between i and j and λ_{ij} is LOS angle as shown in Fig. 2b.

Without loss of generality (WLOG), the target, around which circumnavigation is to be achieved, is assumed to be at the origin. In real-world scenarios, the sensing abilities of agents are often limited. Depending on individual sensing capabilities and initial positions, it is natural that not all the

agents in the group know the target location initially. Keeping this in mind, we partition the agents into two disjoint sets: leaders (\mathcal{L}), who have target information, and the rest are followers (\mathcal{F}).

With this, the objective can be formally stated as: given a group of agents connected over a digraph $\mathcal{G}(\mathcal{V}, \mathcal{E})$ and limited target information availability, our aim is to design a distributed guidance law u_j such that for any initial condition $(x_j(0), y_j(0), \gamma_j(0))$, each agent asymptotically circumnavigates the target. Mathematically, this requires the time-varying distance $r_j(t)$ to converge to the constant target radius R_j for all $j \in \mathcal{V}$, expressed as $\lim_{t \rightarrow \infty} |r_j(t) - R_j| = 0$.

IV. MAIN RESULTS

In this section, we present guidance laws to circumnavigate the target. To formalise the interaction structure among the agents, we introduce the following graph-theoretic definitions.

Definition 1 (Sensing graph): We define the sensing graph $\mathcal{G}_S = (\mathcal{V}, \mathcal{E}_S)$. For nodes $i, j \in \mathcal{V}$, the existence of a directed edge $(i, j) \in \mathcal{E}_S$ implies that agent i can sense agent j .

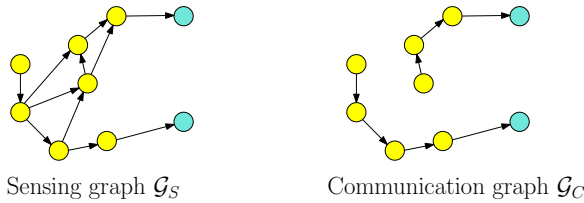


Fig. 3: Leaders and followers are shown in blue and yellow, respectively.

Definition 2 (Communication graph): The communication graph $\mathcal{G}_C = (\mathcal{V}, \mathcal{E}_C)$ is a subgraph of \mathcal{G}_S . In this graph, each agent $i \in \mathcal{V}$ selects as its out-neighbour the closest agent it can sense in \mathcal{G}_S . If multiple nearest candidates exist, the agent may arbitrarily select any one of them (see Fig. 3). Consequently, each follower node has exactly one out-neighbour. Additionally, the leaders are sink nodes.

Hence, \mathcal{G}_C is not unique by construction and may contain multiple disconnected components even for a strongly connected \mathcal{G}_S . Further, we also have the following assumption.

Assumption 1: In the communication graph \mathcal{G}_C , we assume that every follower $f \in \mathcal{F}$ has a directed path to at least one leader in the set \mathcal{L} .

As discussed earlier, the agents in the leader set \mathcal{L} have information about the target location and can guide the followers towards it. Assumption 1 ensures that the information from the leaders propagates to every follower in \mathcal{F} . With this, we now proceed for the guidance law design.

A. Distributed guidance law for followers

In this subsection, we propose a distributed guidance law for all the followers in \mathcal{F} . WLOG, we assume that all the leaders follow suitable guidance laws and converge to stable circular trajectories around the target T (see Fig. 2b). A suitable guidance law for leaders is discussed in the next subsection.

Under Assumption 1, each agent possesses only one out-neighbour. Therefore, for any agent to successfully enter a circular path around the same centre as its out-neighbour (which can either be a leader or another follower) without

using range information, the following set of geometrical conditions must be met, as stated in the next lemma.

Lemma 3: Consider any two agents $i, j \in \mathcal{V}$ such that $(i, j) \in \mathcal{E}_C$. The agents have unicycle kinematics given in eqn. (3). Suppose the agent j traverses a fixed circular trajectory of radius R_j (centred at the target T with angular velocity ω_j). If the following conditions are satisfied, then the agent i is guaranteed to move on a concentric circle with an angular speed ω_j .

- a) the heading angle difference remains constant, i.e. $\dot{\gamma}_j(t) - \dot{\gamma}_i(t) = 0$,
- b) the offset angle between the velocity vector and LOS remains constant, i.e. $\dot{\lambda}_{ij}(t) - \dot{\gamma}_i(t) = 0$.

Proof: The position of agent j can be expressed as $\vec{P}_j(t) = x_j(t) + \iota y_j(t)$. Further, since agent j is circumnavigating the target, its position vector can be written as $\vec{P}_j(t) = R_j \exp(\iota \theta_j(t))$ where the radius R_j is constant and θ_j is the angular coordinate. With reference to Fig. 2b, it follows from the circular geometry that $\gamma_j(t) = \theta_j(t) - \pi/2$. Its velocity vector is then given by $\vec{v}_j(t) = \frac{d}{dt} \vec{P}_j(t) = \iota R_j \dot{\theta}_j(t) \exp(\iota \theta_j(t))$. A constant v_j necessitates that the $\dot{\theta}_j(t)$ is also constant.

Now we analyse the relative motion between the two agents under conditions (a) and (b), and we suitably define two error variables for i :

$$e_{i_1} \triangleq \gamma_j - \gamma_i \quad (5a)$$

$$e_{i_2} \triangleq \lambda_{ij} - \gamma_i \quad (5b)$$

First, we analyse the implication of condition (a). We start by substituting the condition $\gamma_i(t) = \gamma_j(t) - e_{i_1}$ into the expression for $\vec{v}_i(t)$ and simplifying, we get $\vec{v}_i(t) = (v_i/v_j)(\exp(-\iota e_{i_1})) \vec{v}_j(t)$.

So, $\vec{v}_i(t)$ is proportional to $\vec{v}_j(t)$ by a constant, $\alpha \triangleq (v_i/v_j) \exp(-\iota e_{i_1})$. Hence, exploiting the velocity and position relationship, we get $\vec{P}_i(t) = \alpha \vec{P}_j(t) + c$, where c is a constant of integration. Further, $\vec{P}_i(t) = \alpha R_j \exp(\iota \theta_j(t)) + c$ as $\vec{P}_j(t) = R_j \exp(\iota \theta_j(t))$. Note that the equation describes a circular path for agent i of radius $|\alpha|R_j$ and centred at the point c .

Next, on applying condition (b), the angular separation e_{i_2} (as defined in eqn. (5b)) is constant. The LOS vector from i to j is $\vec{r}_{ij}(t) = \vec{P}_j(t) - \vec{P}_i(t)$, which is given by:

$$\vec{r}_{ij}(t) = \vec{P}_j(t) - (\alpha \vec{P}_j(t) + c) = (1 - \alpha) \vec{P}_j(t) - c. \quad (6)$$

Expressed as a function of θ_j , eqn. (6) is $\vec{r}_{ij}(\theta_j) = (1 - \alpha) R_j \exp(\iota \theta_j(t)) - c$.

Then, condition (b), combined with $\gamma_j(t) = \theta_j(t) - \pi/2$, implies that $\arg(\vec{r}_{ij}(\theta_j)) - \theta_j$ must be a constant. For this relationship to hold, its derivative w.r.t. θ_j must be zero:

$$\frac{d}{d\theta_j} (\arg \vec{r}_{ij}(\theta_j(t)) - \theta_j(t)) = 0. \quad (7)$$

Using the identity for the derivative of an argument, $\frac{d}{d\theta_j} (\arg f(\theta_j)) = \text{Img}(f'(\theta_j)/f(\theta_j))$, our condition becomes:

$$\text{Img}\{(\vec{r}_{ij}'(\theta_j)) / (\vec{r}_{ij}(\theta_j))\} - 1 = 0. \quad (8)$$

We compute the derivative $\overrightarrow{R_{ij}}'(\theta_j)$ and the ratio becomes:

$$\frac{\overrightarrow{R_{ij}}'(\theta_j)}{\overrightarrow{R_{ij}}(\theta_j)} = \frac{\iota(1-\alpha)R_j \exp(\iota\theta_j)}{(1-\alpha)R_j \exp(\iota\theta_j) - c}. \quad (9)$$

Substituting the result of the eqn. (9) in the condition from the eqn. (8), we get:

$$\text{Img} \left(\frac{\iota(1-\alpha)R_j \exp(\iota\theta_j)}{(1-\alpha)R_j \exp(\iota\theta_j) - c} \right) - 1 = 0. \quad (10)$$

If we test $c = 0$, the expression simplifies to $\text{Img}(\iota) - 1 = 1 - 1 = 0$, which is true. If $c \neq 0$, the term in the eqn. (10) does not simplify to zero. Therefore, the only possible solution that satisfies the condition for all time is $c = 0$.

Since $c = 0$, the trajectory for i is $\overrightarrow{P_i}(t) = \alpha \overrightarrow{P_j}(t)$. This confirms that agent i circumnavigates the same centre O as agent j and shares the same angular velocity ω_j . ■

Remark 1: When Lemma 3 holds, the triangle $\triangle TP_iP_j$ (see Fig. 2b) is a rigid body. Its side lengths, the radii $R_j = \|P_j(t) - O\|$ and $R_i = \|P_i(t) - O\|$, and the inter-agent distance $r_{ij} = \|P_j(t) - P_i(t)\|$ are all invariant for all $t \in \mathbb{R}$.

Having established in Lemma 3 that circumnavigation for any agent i is characterised by constant values of e_{i_1} and e_{i_2} as defined in eqn. (5). We now transition from this definition to its implementation. In the next result, we present the distributed guidance law for the followers.

Theorem 1: Consider a system of n agents governed by kinematics defined in eqn. (3). Let every leader $l \in \mathcal{L}$ move on a stable circular path such that $\lim_{t \rightarrow t_f} r_l(t) = \bar{r}_l$ and $\dot{\gamma}_l(t) \rightarrow \bar{\omega}_l$. Under Assumption 1, each follower $i \in \mathcal{F}$ is guaranteed to circumnavigate the target T at the same angular rate as the leader at the terminus of its directed path in \mathcal{G}_C under the following distributed guidance law:

$$\dot{\gamma}_i = C_1(\gamma_j - \gamma_i) + C_2 \sin(\lambda_{ij} - \gamma_i), \quad (11)$$

where $C_1, C_2 \in \mathbb{R}^+$.

Proof: The proof proceeds in two stages: first, establishing the stability of a single follower with an out-neighbour that circumnavigates the target, and second, propagating this stability through the communication graph via induction.

Consider a single follower $i \in \mathcal{F}$ having an out-neighbour $j \in \mathcal{L}$ that is already on a stable circular path (see Fig. 2b). Now based on the equilibrium conditions from Lemma 3, the two error variables $e_{i_1} = \gamma_j - \gamma_i$ and $e_{i_2} = \lambda_{ij} - \gamma_i$ are constant at equilibrium. Let the state vector be $\mathbf{e}_i = [e_{i_1} \ e_{i_2}]^T$. The system dynamics are given by:

$$\dot{\mathbf{e}}_i = f(\mathbf{e}_i) = [\dot{e}_{i_1} \ \dot{e}_{i_2}]^T = [f_1 \ f_2]^T. \quad (12)$$

Substituting the values of \dot{e}_{i_1} and \dot{e}_{i_2} in eqn. (12) gives:

$$f(\mathbf{e}_i) = \left[\begin{array}{c} \omega_j - \dot{\gamma}_i \\ \frac{v_j \sin(e_{i_1} - e_{i_2}) + v_i \sin(e_{i_2})}{r_{ij}} - \dot{\gamma}_i \end{array} \right], \quad (13)$$

where $\dot{\gamma}_i = C_1 e_{i_1} + C_2 \sin(e_{i_2})$

Let the equilibrium value of \mathbf{e}_i be $\bar{\mathbf{e}}_i$. The equilibrium values \bar{e}_{i_1} and \bar{e}_{i_2} in eqn. (13) gives the condition:

$$\omega_j = C_1 \bar{e}_{i_1} + C_2 \sin(\bar{e}_{i_2}). \quad (14)$$

With the equilibrium defined, we proceed to analyse its stability properties. We employ Zubov's Theorem for this purpose, as it allows the simultaneous characterisation of the ROA and the stability of the origin. Accordingly, we define a new state variable $\mathbf{z}_i = \mathbf{e}_i - \bar{\mathbf{e}}_i$ to shift equilibrium to origin, where $\mathbf{z}_i = [z_{i_1} \ z_{i_2}]^T$. The new system dynamics are:

$$\dot{\mathbf{z}}_i \triangleq \tilde{f}(\mathbf{z}_i) = \dot{\mathbf{e}}_i = f(\mathbf{z}_i + \bar{\mathbf{e}}_i). \quad (15)$$

Substituting $e_{i_1} = z_{i_1} + \bar{e}_{i_1}$, $e_{i_2} = z_{i_2} + \bar{e}_{i_2}$, and ω_j (from eqn. (14)) into eqn. (13), we obtain:

$$\tilde{f}(\mathbf{z}_i) = [\tilde{f}_{i_1} \ \tilde{f}_{i_2}]^T, \quad (16)$$

where $\tilde{f}_{i_1} = -C_1 z_{i_1} + C_2 (\sin(\bar{e}_{i_2}) - \sin(z_{i_2} + \bar{e}_{i_2}))$ and $\tilde{f}_{i_2} = (v_j \sin(z_{i_1} - z_{i_2} + \bar{e}_{i_1} - \bar{e}_{i_2}) + v_i \sin(z_{i_2} + \bar{e}_{i_2}))/r_{ij} - C_1(z_{i_1} + \bar{e}_{i_1}) - C_2 \sin(z_{i_2} + \bar{e}_{i_2})$.

We choose functions $V(\mathbf{z}_i) = 1 - \exp(-\alpha((z_{i_1})^2 + (z_{i_2})^2))$, where $\alpha \in \mathbb{R}^+$, and $h(\mathbf{z}_i) = -2\alpha[z_{i_1} \ z_{i_2}]^T \tilde{f}(\mathbf{z}_i)$. These functions satisfy the conditions laid down in Lemma 1 in Section II. The function V is continuously differentiable, positive definite in \mathbb{R}^2 ($G = \mathbb{R}^2$), and satisfies eqn. (1). Furthermore, the limit of V as $\|\mathbf{z}_i\| \rightarrow \infty$ is 1.

The constants C_1 and C_2 are selected to ensure that h is positive definite. We then verify the condition:

$$\frac{\partial V}{\partial \mathbf{z}_i} \tilde{f}(\mathbf{z}_i) = -h(\mathbf{z}_i)[1 - V(\mathbf{z}_i)]. \quad (17)$$

For this purpose, we substitute the partial derivative of $V(\mathbf{z}_i)$ and the system dynamics $\tilde{f}(\mathbf{z}_i)$ into the left-hand side of eqn. (17). We obtain:

$$\begin{aligned} \frac{\partial V}{\partial \mathbf{z}_i} \tilde{f}(\mathbf{z}_i) &= \underbrace{2\alpha e^{-\alpha((z_{i_1})^2 + (z_{i_2})^2)} [z_{i_1} \ z_{i_2}]^T}_{\partial V / \partial \mathbf{z}_i} \underbrace{[\tilde{f}_{i_1} \ \tilde{f}_{i_2}]^T}_{\tilde{f}(\mathbf{z}_i)} \\ &= 2\alpha e^{-\alpha((z_{i_1})^2 + (z_{i_2})^2)} (z_{i_1} \tilde{f}_{i_1} + z_{i_2} \tilde{f}_{i_2}). \end{aligned} \quad (18)$$

Recalling proposed $h(\mathbf{z}_i)$ from above and observing that $1 - V(\mathbf{z}_i) = e^{-\alpha((z_{i_1})^2 + (z_{i_2})^2)}$, we can rewrite eqn. (18) as $-h(\mathbf{z}_i)[1 - V(\mathbf{z}_i)]$, which verifies eqn. (17).

As per Lemma 1 stated in Section II, the origin is asymptotically stable. Additionally, the region of attraction is \mathbb{R}^2 . Hence, the origin is GAS. Next, we prove the stability of the entire group.

Now, to prove the stability of the entire group. We define the radial error $d_{j_r}(t) \triangleq r_j(t) - R_j$, where $r_j(t)$ is the distance from the target and R_j is a constant value. Leaders $l \in \mathcal{L}$ converge by definition in theorem statement, so $\lim_{t \rightarrow t_f} d_{l_r}(t) = 0$ and $\dot{\gamma}_l \rightarrow \bar{\omega}_l$.



Fig. 4: A directed path within \mathcal{G}_C terminating at the leader l_m .

Now, consider a path $l_m \leftarrow f_1 \leftarrow \dots \leftarrow f_k$ as shown in Fig. 4. Assume follower f_k has converged to a stable circular path with speed $\bar{\omega}_{l_m}$. For the next follower f_{k+1} , the agent f_k acts as a stable leader. Applying the result from stage one of the proof, f_{k+1} must also converge to a circular path and match the angular speed of f_k (and thus of l_m).

By Assumption 1, every follower has a path to a leader, this inductive argument cascades to all $f \in \mathcal{F}$. Hence, all agents converge to their respective radii and angular speeds. ■

This concludes the analysis for followers. Since leaders possess more information, their circumnavigation task is simpler. The next subsection discusses a specific approach for leaders.

B. Guidance law for leaders

We begin by recalling that the leaders have information about the target and aim to circumnavigate it, as do the followers. In the proposed design methodology for the followers, the leaders in \mathcal{L} are assumed to follow circular trajectories. Keeping practical implementability in mind, we employ a guidance law for leaders that drives them toward suitable trajectories within a feasible, prescribed time.

We employ CC trajectories as they offer sufficient control over β and r_B (see Fig. 1) and enable leaders to autonomously select α , β , and r_B , thereby facilitating collision avoidance. For the same, we leverage a geometric result with constant inputs from our prior work in [23] to implement these trajectories (see Lemma 2). This formulation ensures that for any feasible r_A , a unique r_B exists to connect a and b via two tangent circular arcs. Consequently, any initial configuration can be steered to the desired target path using only two circular arcs.

Having concluded the theoretical analysis and proofs, we now proceed to validate these findings. The subsequent sections detail the simulations and experimental results.

V. SIMULATION RESULTS

In this section, we validate the proposed guidance law via numerical simulations using two static graph topology setups: a single-leader case and a two-leader case. In all plots, leaders are represented by blue and followers by yellow.

TABLE I: Simulation's initial conditions (in SI units).

Agent	Case 1			Case 2		
	P	V	γ	P	V	γ
1	(2,2)	18	-2.44	(2,1)	28	-2.53
2	(-24,-15)	36	-1.48	(34,-5)	35	-1.57
3	(-20,35)	74	0.61	(-10,15)	50	-0.52
4	(30,-45)	99	-1.19	(10,-25)	18	-1.05
5	(-29,-11)	24	-1.34	(-25,-15)	22	-1.31
6	NA	NA	NA	(10,23)	40	-1.43

Case 1: Single leader configuration

Fig. 5a depicts the communication topology for five agents converging to circular orbits. The initial conditions are given in TABLE I. Consistent with Theorem 1, agents converge to circular orbits (Fig. 5b) with stabilised horizontal distances (Fig. 5c). Moreover, Fig. 5d shows all control inputs converging to a unified value, confirming the formation of a single invariant rotating structure.

Case 2: Two leader configuration

Fig. 6a shows the topology for a six-agent, two-leader system. Initial conditions are given in TABLE I. As predicted, agents converge to circular paths (Fig. 6b) with constant target separation (Fig. 6c). Control inputs (Fig. 6d) reveal that ω_2, ω_3 synchronize with ω_1 , while ω_4, ω_5 synchronize with ω_6 . This results in two distinct invariant rotating bodies: a triangle connecting agents 1–3 and another connecting agents 4–6. These simulations confirm theoretical predictions.

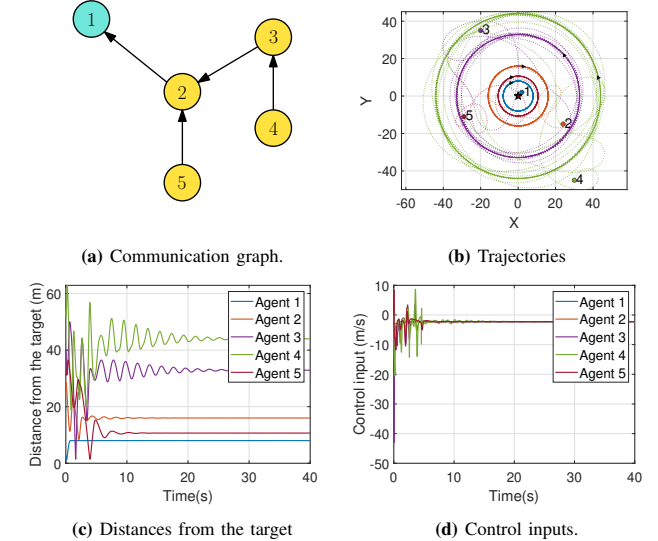


Fig. 5: Case 1.

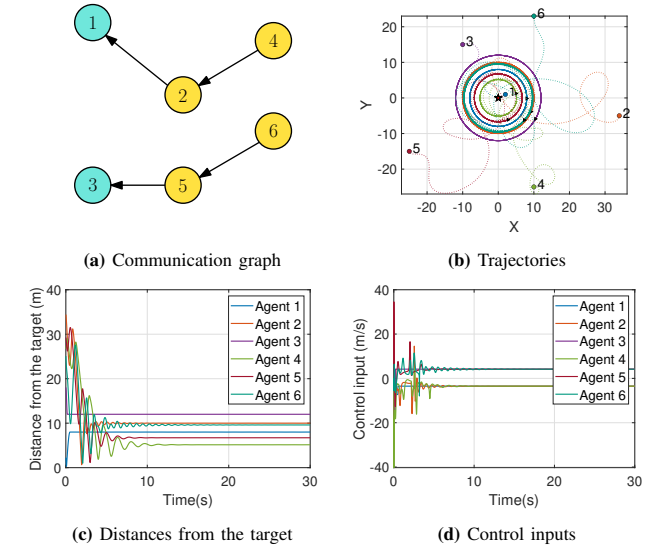


Fig. 6: Case 2.

VI. EXPERIMENTAL VALIDATION

In this section, we demonstrate practical feasibility through hardware experiments with a leader-follower pair of ground mobile robots. These tests validate theoretical predictions and assess the robustness against real-world challenges, including sensor noise, communication delays, and actuation constraints.

The testbed comprises two infrared reflective marker-equipped TurtleBot3 Burger robots ($v_{max} = 0.22\text{m/s}$). They

are tracked by a six-camera OptiTrack system providing sub-millimetre accuracy at 120Hz. A centralised node computes relative angles ($\gamma_j - \gamma_i$ and $\lambda_{ji} - \gamma_i$) from the tracking data and transmits commands via WiFi. To ensure faster convergence, the leader was pre-positioned on a 0.7 m radius circle, while the follower started from an arbitrary condition.

The leader's and follower's linear speeds were set to 0.105 m/s and 0.15 m/s, respectively. Their respective initial positions were (0.7 m, 0 m) and (0.87 m, 0.16 m), with initial headings of 90° and 139°.

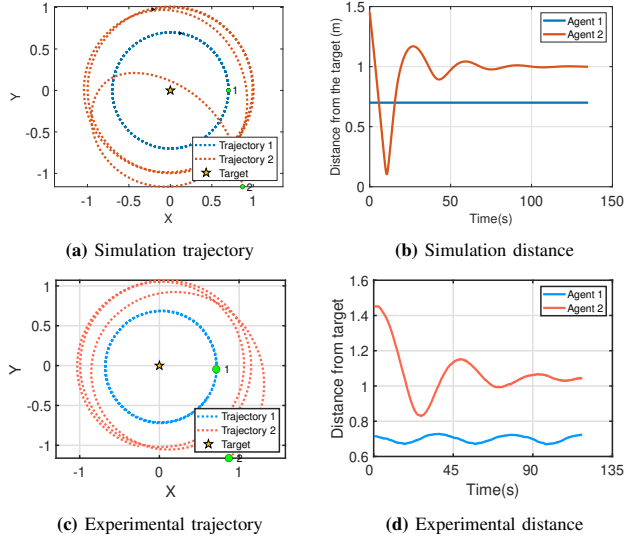


Fig. 7: Comparison of simulation and experimental results.

In Fig. 7 (Agent 1: leader, Agent 2: follower), trajectories in both simulation (Fig. 7a) and experiment (Fig. 7c) confirm that the follower successfully achieves concentric circular motion. While the simulated follower settles at 0.999 m (Fig. 7b), experimental distance settles between 0.96 m and 1.04 m (Fig. 7d). The leader's experimental distance exhibits noise induced waviness (0.66–0.74 m) around the 0.7m target, but remains bounded. Due to space constraints, only the faster-follower scenario is presented. The video link for the experiment is <https://youtu.be/-4YHJBETVX0>.

VII. CONCLUSION

In this paper, we present a bearing based distributed guidance law to achieve circumnavigation of a stationary target by a group of n heterogeneous autonomous agents, modelled as unicycles. The agents are assumed to have constant linear speeds; this further under-actuated the model but enhances its applicability. In the given framework, only a subset of the agents know the target location, referred to as *leaders* while the rest are called *followers*. For the leaders, we employ circular trajectories for ensuring finite-time target circumnavigation. A distributed bearing-based guidance law is designed for the followers, as presented in Theorem 1. The proposed design ensures GAS even by controlling only the angular speeds. The results are illustrated through numerical simulations. The practical implementability has also been demonstrated through realworld hardware experiments performed on TurtleBots using an OptiTrack motion capture system.

REFERENCES

- [1] N. E. Leonard, D. A. Paley, F. Lekien, R. Sepulchre, D. M. Fratantoni, and R. E. Davis, "Collective motion, sensor networks, and ocean sampling," *Proceedings of the IEEE*, vol. 95, no. 1, pp. 48–74, 2007.
- [2] B. Jha, R. Tsalik, and T. Shima, "Lemniscate-based guidance for directed reconnaissance," *Journal of Guidance, Control, and Dynamics*, vol. 0, no. 0, pp. 1–11, 0.
- [3] I. A. Aromoye, H. H. Lo, P. Sebastian, G. E. M. Abro, and S. L. Aiyinla, "Significant advancements in uav technology for reliable oil and gas pipeline monitoring," *Computer Modeling in Engineering & Sciences (CMES)*, vol. 142, no. 2, 2025.
- [4] X. Li, X. Liu, S. Wu, J. Zhang, and L. Ma, "Bearing-based finite-time fire positioning and fire extinguishing circumnavigation control for multiple intelligent firefighting robots," *IEEE Transactions on Control Systems Technology*, 2025.
- [5] J. Wang, B. Ma, and K. Yan, "Mobile robot circumnavigating an unknown target using only range rate measurement," *IEEE Transactions on Circuits and Systems II: Express Briefs*, vol. 69, no. 2, pp. 509–513, 2021.
- [6] A. Sinha and Y. Cao, "3-d nonlinear guidance law for target circumnavigation," *IEEE Control Systems Letters*, vol. 7, pp. 655–660, 2022.
- [7] D. Milutinović, D. Casbeer, Y. Cao, and D. Kingston, "Coordinate frame free dubins vehicle circumnavigation," in *2014 American Control Conference*. IEEE, 2014, pp. 891–896.
- [8] —, "Coordinate frame free dubins vehicle circumnavigation using only range-based measurements," *International Journal of Robust and Nonlinear Control*, vol. 27, no. 16, pp. 2937–2960, 2017.
- [9] F. Dong, Y. Hsu, and K. You, "Circumnavigation of an unknown target using range-only measurements in gps-denied environments," in *2019 IEEE 15th International Conference on Control and Automation (ICCA)*. IEEE, 2019, pp. 411–416.
- [10] A. Hashemi, Y. Cao, D. W. Casbeer, and G. Yin, "Unmanned aerial vehicle circumnavigation using noisy range-based measurements without global positioning system information," *Journal of Dynamic Systems, Measurement, and Control*, vol. 137, no. 3, p. 031003, 2015.
- [11] R. Sepulchre, D. A. Paley, and N. E. Leonard, "Stabilization of planar collective motion with limited communication," *IEEE Transactions on Automatic Control*, vol. 53, no. 3, pp. 706–719, 2008.
- [12] J. A. Marshall, M. E. Broucke, and B. A. Francis, "Formations of vehicles in cyclic pursuit," *IEEE Transactions on Automatic Control*, vol. 49, no. 11, pp. 1963–1974, 2004.
- [13] A. Sinha and D. Ghose, "Generalization of nonlinear cyclic pursuit," *Automatica*, vol. 43, no. 11, pp. 1954–1960, 2007.
- [14] T. Tripathy and T. Shima, "On convergence results for nonlinear cyclic pursuit strategies," *Automatica*, vol. 159, p. 111315, 2024.
- [15] J. L. Ramirez-Ribero, M. Pavone, E. Frazzoli, and D. W. Miller, "Distributed control of spacecraft formations via cyclic pursuit: Theory and experiments," *Journal of guidance, control, and dynamics*, vol. 33, no. 5, pp. 1655–1669, 2010.
- [16] M. I. El-Hawary and M. Maggiore, "Distributed circular formation stabilization for dynamic unicycles," *IEEE Transactions on Automatic Control*, vol. 58, no. 1, pp. 149–162, 2012.
- [17] G. S. Seyboth, J. Wu, J. Qin, C. Yu, and F. Allgöwer, "Collective circular motion of unicycle type vehicles with nonidentical constant velocities," *IEEE Transactions on Control of Network Systems*, vol. 1, no. 2, pp. 167–176, 2014.
- [18] R. Zheng, Z. Lin, M. Fu, and D. Sun, "Distributed control for uniform circumnavigation of ring-coupled unicycles," *Automatica*, vol. 53, pp. 23–29, 2015.
- [19] X. Yu, X. Xu, L. Liu, and G. Feng, "Circular formation of networked dynamic unicycles by a distributed dynamic control law," *Automatica*, vol. 89, pp. 1–7, 2018.
- [20] X. Yu, L. Liu, and G. Feng, "Distributed circular formation control of nonholonomic vehicles without direct distance measurements," *IEEE Transactions on Automatic Control*, vol. 63, no. 8, pp. 2730–2737, 2018.
- [21] A. Sen, S. R. Sahoo, and M. Kothari, "Circumnavigation on multiple circles around a nonstationary target with desired angular spacing," *IEEE Transactions on Cybernetics*, vol. 51, no. 1, pp. 222–232, 2019.
- [22] H. K. Khalil and J. W. Grizzle, *Nonlinear systems*. Prentice hall Upper Saddle River, NJ, 2002, vol. 3.
- [23] A. K. Rao, K. P. Singh, and T. Tripathy, "Curvature bounded trajectories of desired lengths for a dubins vehicle," *Automatica*, vol. 167, p. 111749, 2024.